OPTIMIZATION OF LINEAR INDUCTION RADIOGRAPHY ACCELERATOR WITH ELECTRON BEAM WITH ENERGY VARIATION

Yuan Hui Wu† and Yu-Jiuan Chen

Lawrence Livermore National Laboratory, Livermore CA, USA

Abstract

The current interest for the next generation linear induction radiography accelerator (LIA) is to generate multiple, high peak current, electron beam pulses. The beam energy and current may vary from pulse to pulse. Consequently, the transport and control of multi-pulsing intense electron beams through a focusing lattice over a long distance on such a machine becomes challenging. Simulation studies of multi-pulse LIAs using AMBER [1] and BREAKUP Code [2] are described. These include optimized focusing magnetic tune for beams with energy and current variations, and steering correction for corkscrew motion. The impact of energy variation and accelerating voltage error on radiograph performance are discussed.

INTRODUCTION

Controlling beam transport is essential for accelerator operation and future induction accelerator design. In this study, see Figure 1, we simulated a conceptual linear induction accelerator. The nominal incoming 2-MeV, 2-kA electron beam exiting from the diode injector has a uniform KV distribution with a 5 cm edge radius (r = 5 cm) and an 800π mm-mrad edge normalized emittance ($\varepsilon = 800\pi$ mm-mrad). The incoming beam has a small energy variation ($d\gamma/\gamma$), which varies from -5% to 5% with respect to the nominal beam energy.
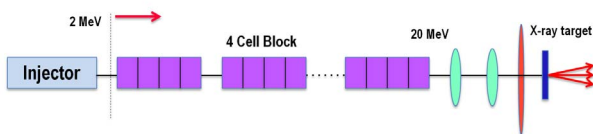

Figure 1: The conceptual accelerator configuration used in the simulations. The model has 72 cells arranged into 18 blocks, and an intercell gap of 50 cm.

† wu39@llnl.gov

The accelerator consists of 18 4-cell blocks, which accelerate the electron beam to 20 MeV. The intercell separation is 50 cm. The accelerating voltage in each accelerator cell (see Figure 2) is 250kV(1+dV/V), where dV/V is varies from -5% to 5%. The downstream beamline consists of two focusing solenoids and a final focusing solenoid.
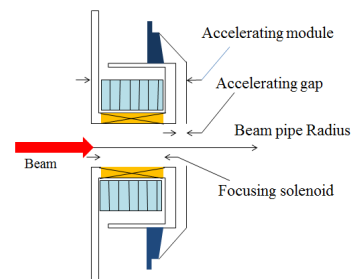

Figure 2: Schematic of simulated 250kV accelerating cell.

ELECTRON BEAM TRANSPORT AND TUNE OPTIMIZATION

To preserve the beam quality, the beam envelope oscillation needs to be minimized [3]. As shown in Figure 3, the solenoid magnetic tune is optimized to reduce the envelope oscillation for a nominal electron beam. Transport of the electron beam with different initial energy variation and accelerating voltage variation is simulated using the same magnetic tune. For the beam produced with an initial energy variation, the beam current also varies according the Child-Langmuir's law. Electron beam slices with initial energy variations from -5% to 5% and accelerating voltage errors from -5% to 5% were simulated (Fig. 3). The beam slice with larger initial energy variation has larger envelope oscillation. Likewise, the beam slice transport through accelerator with large voltage error experiences larger envelope oscillation.

By using AMBER slice PIC code, an electron beam pulse with a given different initial energy variation was simulated by dividing the pulse into 20 slices. Each slice represents a por-

tion of the pulse with the initial energy varying linearly from the head to the tail. The accelerating voltage waveform also varied by assuming the voltage waveform linearly increases from the head to the tail. Each slice is then accelerated by a different accelerating voltage according to the slice time. The time integrated emittance and beam size were calculated by accumulating all the particles from all slices. As show in Figure 4, the beam size and emittance of the beam at the accelerator exit increase for the beam pulse with a larger initial energy variation or for a larger accelerating voltage error.
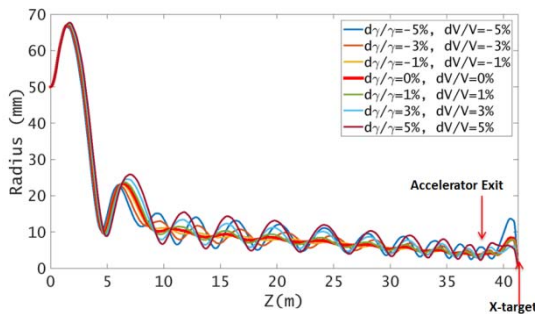

Figure 3: Envelopes for electron beam with different initial energy variation dγ/γ and accelerating voltage error dV/V. The beam envelope for the nominal beam is given by the thick red line.
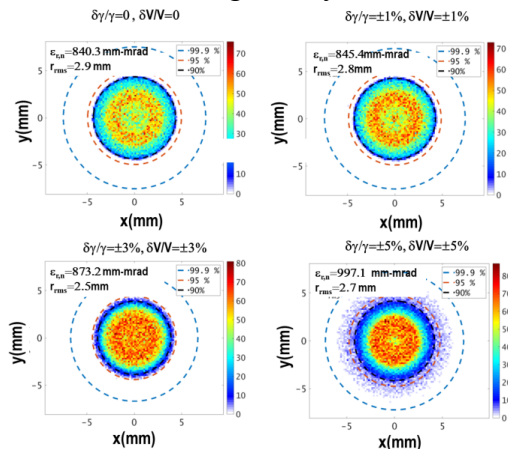

Figure 4: Calculated electron beam size at the accelerator exit for various initial energy variations and accelerating voltage errors.

FINAL FOCUS OPTIMIZATION

Flash radiography imaging requires the electron beam be tightly focused onto an x-ray converter target. Multi-Objectives Global optimization algorithm (Genetic Algorithm) [4] is used to optimize the magnetic setting for both the

minimum integrated emittance and the desired time integrated spot size at the target (Figure 5). Note that the back-streaming ion effect [5], not included in this optimization study, can lead to spot size increase, [6] However, this optimization technique can still be used to optimize the spot size with back-streaming effect.

The final time integrated phase spaces are shown in Figure 6. The time integrated emittance and spot size at the target increase for larger initial energy spread and accelerating voltage. The radiography resolution depends on the spot size defined by the 50% modulation transfer function (MTF) [7]. We used the time-integrated profiles to calculate the 50% MTF spot sizes for all the cases we studied, which are shown in Table 1. Both the initial energy spread and the accelerating voltage error have a large impact on the 50% MTF spot size.

The forward x-ray doses for all cases we studied were calculated using the scaling law given in Reference [8]. As shown in Table 1, the forward x-ray dose is about the same for all the cases we studied. Neither the initial energy spread nor the accelerating voltage has impact on the forward x-ray dose.

Table 1: Summary of Beam Parameters at the Target

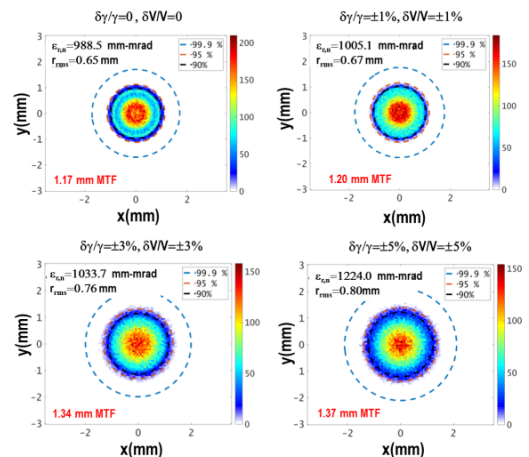| Injector energy spread δγ/γ (± %)	Accelerator Voltage variation δV/V (± %)	R_rms (mm)	Normalized Lapostolle Emittance (mm-mrad)	50% MTF (mm)	ΔD/D (%)
0	0	0.65	988	1.17	0
1	1	0.67	1005	1.20	0.2
2	2	0.72	1026	1.25	1.0
3	3	0.76	1034	1.34	1.8
5	5	0.80	1224	1.37	0.6

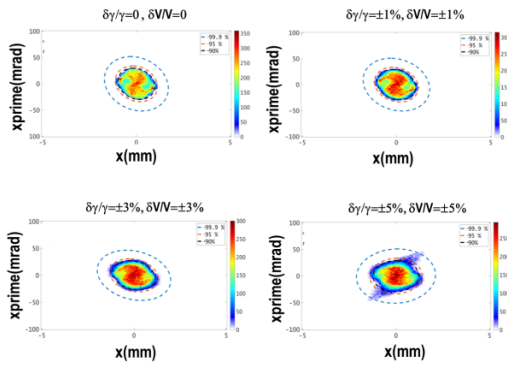Figure 5: Calculated electron beam size at the target.

Figure 6: Calculated time integrated electron beam phase space (x-x') at the target.

CORKSCREW MOTION MINIMIZATION

Corkscrew motion [9] is caused by misalignment and chromatic aberration of the transport system. The corkscrew can be minimized by removing the error field's k_c components for beam slices over a wide range of energy. The tuning-V algorithm can successfully minimize corkscrew motion. In practice, using the algorithm to minimize both the corkscrew and beam centroid displacement is not easy. By using the BREAKUP code, we studied optimizing the steering magnet setting to remove both the corkscrew motion and the centroid displacement. Solenoid magnets were randomly misaligned with solenoid displacement $3\sigma = 2$ mm and solenoid tilt $3\sigma = 2$ mrad. The accelerator voltage error dV/V is ±5%. The beam's initial dγ/γ is ± 5%, and its initial offset $x_{off} = y_{off} = 0.5$ mm. Two steering coil pairs are used to eliminate corkscrew motion and to steer the beam back to machine axis at the accelerator exit. The steering magnet setting was optimized using the global optimization algorithm (genetic algorithm). The results given in Figure 7 show that the optimization scheme can effectively reduce both the corkscrew and centroid displacement.

SUMMARY

Beam transport on a conceptual induction accelerator was optimized with the Global optimization algorithm. The effect of energy variation of the electron beam on the radiography performance was evaluated. Energy variation
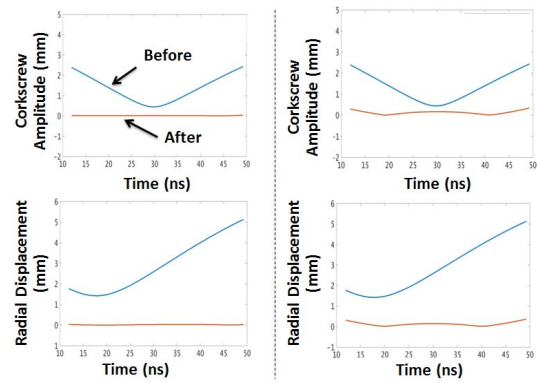

Figure 7: Corkscrew optimization using two pairs of steering coils at the middle of accelerator (left) and at the beginning of accelerator (right).

has large impact on the 50% MTF spot size but not on the forward x-ray dose. The optimization scheme can also be used to set the magnetic strength of two steering coil pairs to reduce corkscrew motion and transverse centroid displacement.

ACKNOWLEGEMENTS

REFERENCES

[1] J. L. Vay, W. Fawley, Amber code, 2000.

[2] Y.-J Chen, W. Fawley, BREAKUP Code.

[3] M. Reiser, Theory and design of charged particle beams, New York. NY: Wiley, 1994.

[4] K. Deb. John Wiley and Sons, Chichester, 2001.

[5] G. J. Caporaso and Y.-J Chen, UCRL-JC-130594, LLNL.

[6] Y. Wu, Y-J. Chen, presented at NAPAC2016, Chicago, IL, USA, October 2016, this conference.

[7] C. Ekdahl, *J. Opt. Soc. Am.*, vol. 28, No. 12.

[8] Y.-J Chen, April 2000. UCRL-ID-140189, LLNL

[9] Y.-J. Chen, *Nucl. Inst. Meth. A*, vol. 398:139, 1997.